Effects of the target spin on the reaction mechanism of the $^{16}O + ^{63}Cu$ system

J. M. B. Shorto,[1] E. Crema,[1,*] R. F. Simões,[1] D. S. Monteiro,[1] J. F. P. Huiza,[1] N. Added,[1] and P. R. S. Gomes[2]

[1]*Departamento de Física Nuclear, Instituto de Física da Universidade de São Paulo, Caixa Postal 66318, São Paulo 05315-970, SP, Brazil*

[2]*Instituto de Física, Universidade Federal Fluminense, Av. Litorânea s/n, Gragoatá, Niterói, Rio de Janeiro 24210-340, Brazil*

(Received 27 March 2008; published 19 December 2008)

Precise quasielastic and α-transfer excitation functions, at $\theta_{lab} = 161^{\circ}$, have been measured at energies near the Coulomb barrier for the $^{16}O + ^{63}Cu$ system. This is the first time reported quasielastic barrier distribution for a medium odd-A nucleus target deduced from the data. Additional elastic scattering angular distributions data available in the literature for this system were also used in the investigation of the role of several individual channels in the reaction dynamics, by comparing the data with free-parameter coupled-channels calculations. In order to do so, the nucleus-nucleus bare potential has a double-folding potential as the real component and only a very short-range imaginary potential. The quasielastic barrier distribution has been shown to be a powerful tool in this analysis at the barrier region. A high collectivity of the ^{63}Cu was observed, mainly due to the strong influence of its $5/2^-$ and $7/2^-$ states on all reaction channels investigated. A striking influence of the reorientation of the ground-state target-spin on the elastic cross sections, taken at backward angles, was also observed.

DOI: 10.1103/PhysRevC.78.064610 PACS number(s): 25.60.Pj, 25.70.Mn, 25.70.Jj, 24.10.Eq

I. INTRODUCTION

It is a well-known fact that the fusion of heavy nuclei at energies around the Coulomb barrier can be strongly influenced by the coupling between intrinsic degrees of freedom of the colliding nuclei and their relative motion. This effect usually enhances the fusion cross section at energies below the Coulomb barrier, when compared with theoretical predictions based on single barrier penetration models [1–7]. The effect of the couplings corresponds to the replacement of the single barrier by a distribution of barriers, which can be extracted directly from the experimental fusion excitation function [8,9]. An alternative and simpler method to derive barrier distributions has been proposed [10], by utilizing the quasielastic excitation function, measured at backward angles. Quasielastic process is defined as the sum of elastic, inelastic and transfer reactions, and due to the reaction flux conservation, it is complementary to fusion, at near barrier energies. The quasielastic barrier distribution, equivalent to fusion distribution [10–14], is obtained from the expression [10]

$$D^{qel}(E) = -\frac{d}{dE}\left(\frac{d\sigma^{qel}(E)}{d\sigma^{Ruth}(E)}\right). \quad (1)$$

Barrier distributions have been very successful in revealing deeper details of the reaction dynamics at near barrier energies than excitation functions [9]. However, most of the systems investigated by this method are concerned with even-even mass nuclei and heavy targets. There are very few available data for light and medium-weight systems, particularly for odd targets, for which the ground state spin may play an important role in the coupling scheme. After measuring quasielastic barrier distributions for some light and medium-weight even-even systems, like $^{16,18}O + ^{58}Ni$ [14], $^{16,18}O + ^{92}Mo$ [16], and $^{16}O + ^{64}Zn$ [17], in this paper our group presents results of the investigation of how the nuclear structure details of the odd-mass target nucleus influence the reaction mechanism in the system $^{16}O + ^{63}Cu$ at energies near and below the Coulomb barrier.

The ^{63}Cu nucleus has a large static ground-state deformation ($Q = -0.211$ b) and spin $3/2^-$. These features might have important role in the quantum interference of different reaction channels in this system, since it is well known that reaction mechanisms of systems with an odd-mass nucleus can be affected by the spin of such nucleus. The diffraction minima in the elastic scattering of light particles by odd-mass targets can be dominated by the ground-state target-spin reorientation process [18–20]. When more massive projectiles are involved, the elastic scattering at large angles can also be dominated by the reorientation process of the odd-mass nucleus [21,22]. The influence of the reorientation of excited states of even-mass nuclei on the reaction mechanism has also been investigated [23].

However, in most of the reported works on the investigation of reorientation effects, particularly with systems involving odd-nuclei, coupled-channels calculations were performed including only very few channels in the coupling matrix. Therefore, in those calculations it was required the introduction of an imaginary potential to account for the channels not included in the coupling scheme. Their common conclusion was that if the reorientation effects were taken into account, the strength of the optical model imaginary potential could be reduced and good fits to the data could be obtained. Of course, if all open reaction channels were included in the calculations, no imaginary potential at surface would be required.

The aim of the present work was not to obtain the best fit to our original and to the other available data for this system, by changing several potential parameters, but rather to investigate the relative role of all reaction channels in the quantum competition by the reaction flux. As the bare nuclear interaction between the projectile and the target, we used the parameter-free double-folding Sao Paulo potential (SPP) [24,25]. The only imaginary potential used was a very

*crema@dfn.if.usp.br

short-range imaginary potential, to simulate the incoming wave boundary condition to account for the fusion process. Then we started coupling, one by one, all excited states of projectile and target for which the experimental $B(E2)$ values were available in the literature. If the nuclear structure parameters were available in the literature for all inelastic and transfer channels, no superficial imaginary potential would have to be included in the calculations and good data fit should be obtained. As this was not the present situation, we performed theoretical predictions to be compared with data, rather than a fit to the data. With such interesting procedure, it becomes clear the physical origin of the imaginary optical potential commonly used in the usual calculations.

The ideal situation for the theoretical approach described above is the availability of complete high precision data sets for elastic, inelastic, transfer and fusion processes. In order to minimize the lack of such complete data set for the $^{16}O + ^{63}Cu$ system, we have measured α-transfer and high precision quasielastic backward angle excitation functions, from which a representation of the quasielastic barrier distribution was also deduced. In the analysis, these original data were added to available but not published [26] data of elastic scattering angular distributions for this system. There are no inelastic scattering data in the literature for this system.

In the next section we present the experimental details and results. In section three we describe the coupled-channels calculations and the comparison of their results with the data. Finally, a summary is made and conclusions are presented.

II. EXPERIMENTAL METHOD AND RESULTS

The experiment was carried out with ^{16}O beams from the 8 UD Pelletron Accelerator at the University of São Paulo with laboratory energies ranging from 30.0 to 48.0 MeV and beam intensities from 10 to 100 pnA. An energy step of 0.5 MeV was used in almost the entire energy range. A 90° analyzing magnet defined the beam energy with an uncertainty of the order of 40 keV. Before starting to take data, the analyzing magnet was properly recycled, and the measurements were taken only with decrements in the beam energy. The self-supporting target was 80 μg/cm^{2}of isotopically enriched ^{63}Cu (99.86%).

The identification of the scattered nuclei was extracted from E-ΔE spectra, where the ΔE signal was supplied by the energy loss in the gas of a conventional proportional counter placed at $\theta_{lab} = 161^\circ$ ($\theta_{c.m.} \sim 166^\circ$). The proportional counter was operated with a gas mixture P-10 at a pressure of 15 torr. Behind the gas detector there was a silicon surface barrier detector to determine the residual energy. Figure 1 shows a typical E-ΔE spectrum, taken at $E_{lab} = 40$ MeV. The resolution in Z allowed the identification of all quasielastic events with $Z = 6, 7, 8$, and, consequently, the extraction of the experimental excitation functions for these processes. On the other hand, in the $Z = 8$ region of the spectra, the energy resolution was not enough to separate the elastic scattering from the lowest target excited state inelastic scattering, since in backward angle measurements a large solid angle is required to measure a high precision excitation function. But, as we were interested only in the inclusive quasielastic scattering data, this problem did not disturb our analysis. The energy

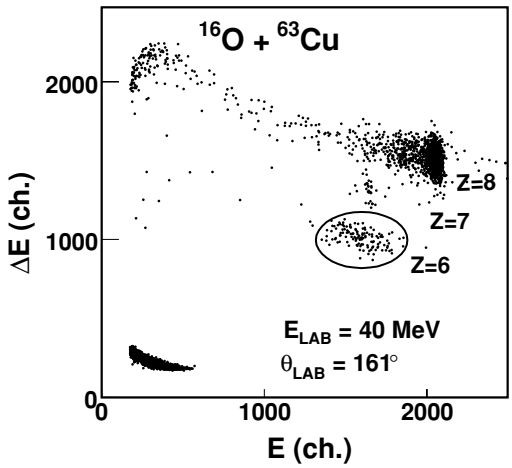

FIG. 1. The E-ΔE spectrum taken at 40 MeV and 161°, where E and ΔE are in channels.

cutoff used in the counting procedure guarantees that inelastic events with excitation energies up to 6 MeV, if they occur, could be taken into account. The quasielastic cross section was calculated by summing the counts of interest of the $Z = 6, 7$, and 8 events. Three silicon detectors were placed at forward angles ($\pm 30^\circ$ and -45°) for normalization purposes. So, three quasielastic excitation functions were calculated using their outcomes and they were found to be coincident inside the experimental uncertainties. The uncertainties associated with the measurements are lower than 1%, except for the highest energies, where they are approximately 3%.

The measured quasielastic excitation function is shown in Fig. 2, and its correspondent experimental quasielastic barrier distribution, which is shown in Fig. 3, was derived using a point-difference approximation, with laboratory energy steps of 2.0 MeV. As these quasielastic inclusive data are

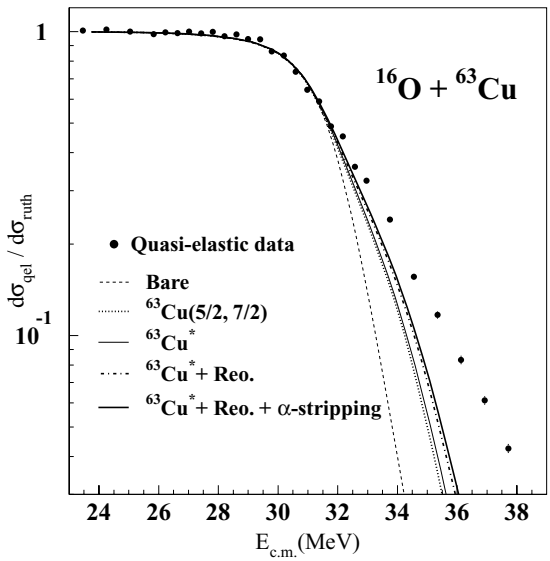

FIG. 2. The experimental quasielastic excitation function, at 161°. The curves are results of coupled-channel calculations discussed in the text. The $E_{c.m.}$ was corrected by the correspondent centrifugal barrier.

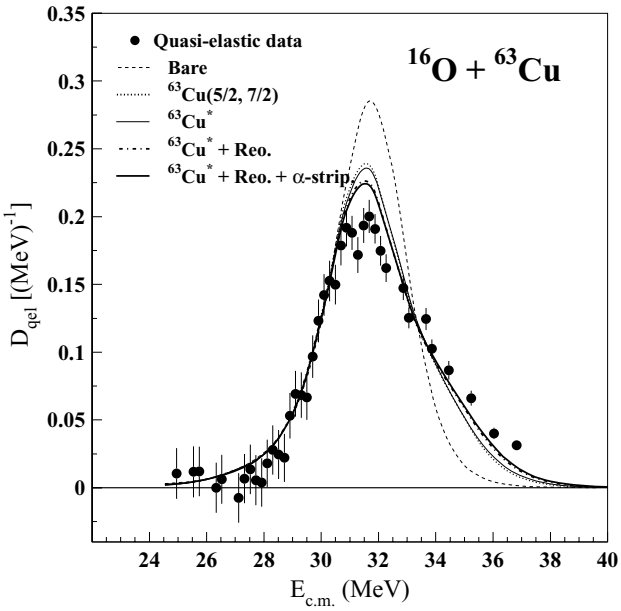

FIG. 3. The experimental barrier distribution, D^{qe}, deduced from quasielastic excitation function. The dotted line corresponds to the barrier penetration model (BPM) calculation. The full line is the result of coupled-channel calculations discussed in the text. The $E_{c.m.}$ was corrected by the correspondent centrifugal barrier.

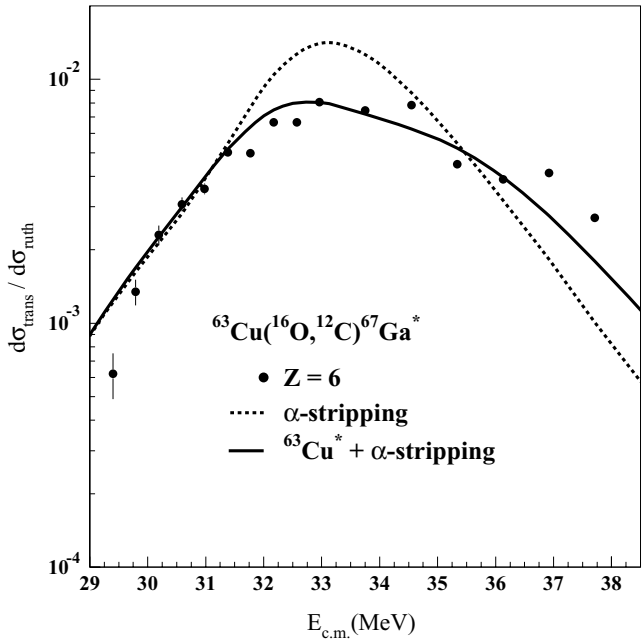

FIG. 4. The excitation function, at 161°, for the transfer events leading to projectile-like events with $Z = 6$. The curves are the results of coupled-channel calculations discussed in the text.

complementary to the fusion process, the barrier distribution presented in the Fig. 3 can be directly compared to the fusion barrier distribution of this system. In order to facilitate this comparison, the $E_{c.m.}$ energies of Figs. 2 and 3 were corrected by the centrifugal potential energy at 161°, as suggested by Rowley *et al.* [11]. The theoretical barrier distributions presented in the next section were deduced from the theoretical excitation function using the same procedure and energy steps. The excitation function for the transfer events leading to projectile-like particles with $Z = 6$ is presented in Fig. 4.

III. COUPLED-CHANNELS CALCULATIONS

A crucial first step procedure when performing coupled-channels calculations (CCC) is the choice of a bare potential to simulate the nuclear interaction between projectile and target nuclei, since the results are bare-potential dependent [27]. It has already been demonstrated that double-folding potentials may be considered as a reliable starting point for CCC involving both stable and unstable nuclei [27–29]. In the present work, the real bare interaction was represented by the parameter-free double-folding potential that is used to construct the more general São Paulo potential (SPP) [24,25]. As the fusion process in not explicitly included in the calculations, an imaginary potential had to be used. In order to account for the fusion process, and not disturb the competition between the superficial channels involved in the calculations, we used a very short-range and fixed imaginary potential: $V_i = 80$ MeV, $r_i = 0.8$ fm, and $a_i = 0.6$ fm, as suggested by Ref. [30]. This imaginary potential simulates the incoming wave boundary condition and the following calculations are not very sensitive to its parameters. In our calculations, we used the version FRXP.3i of FRESCO code [31], which allows the coupling of several channels. Actually, in the following calculations, up to 12 transitions were coupled.

A. Quasielastic excitation function and barrier distribution

The dashed line in Fig. 2 represents the quasielastic excitation function generated by the bare potential, without any couplings. For energies below the Coulomb barrier (31.5 MeV), this curve gives a good prescription of the quasielastic excitation function, indicating that the elastic scattering is the dominant process in this energy region.

Indeed, this agreement indicates that the bare potential describes well the interaction between the cores of the two nuclei. However, for energies above 32 MeV, this calculation is not able to describe the data. The explanation for this failure is the opening of other reaction channels at high energies. From Eq. (1), the experimental and theoretical excitation functions were employed to deduce their corresponding barrier distributions, which are shown in Fig. 3. The dashed curve represents the theoretical quasielastic barrier distribution without any couplings. One can notice that although the excitation function indicates a good agreement between uncoupled calculation and data up to 32 MeV, the barrier distribution shows that this agreement is valid only up to 30 MeV, and that the influence of other reaction channels is important even at energies below the Coulomb barrier. This fact is an evidence of quantum-tunneling effects that occurs in this energy region. So, it becomes clear that the quasielastic barrier distribution is a powerful and sensible tool for investigating reaction mechanisms at energies around the Coulomb barrier.

The next step in our calculations was to include in the coupling matrix, one-by-one, the lowest excited states of the

TABLE I. All inelastic transitions of ^{63}Cu used in the coupled channel calculations.

^{63}Cu				
$I_f \rightleftarrows I_i$	E_γ (KeV)	$B(E2)$(W.u.)	$\langle I_f \vert E\lambda \vert I_i \rangle$	δ_2 (fm)
$\frac{3}{2} \rightleftarrows \frac{1}{2}$	669.62(5)	15.20(18)	21.28 e^2 fm^4	0.728
$\frac{3}{2} \rightleftarrows \frac{5}{2}$	962.06(4)	15.70(17)	37.45	1.280
$\frac{3}{2} \rightleftarrows \frac{7}{2}$	1327.03(8)	12.7(7)	38.90	1.330
$\frac{3}{2} \rightleftarrows \frac{5}{2}$	1412.08(5)	1^{+4}_{-1}	9.45	0.323
$\frac{1}{2} \rightleftarrows \frac{5}{2}$	742.25(10)	6^{+23}_{-6}	23.15	0.793
$\frac{3}{2} \rightleftarrows \frac{3}{2}$	1547.04(6)	3.70(12)	−14.84	−0.510
$\frac{3}{2} \rightleftarrows \frac{7}{2}$	1861.3(3)	1.4(5)	12.91	0.450
$\frac{7}{2} \rightleftarrows \frac{11}{2}$	1350.1(4)	10(3)	42.27	1.447
$\frac{3}{2} \rightleftarrows \frac{7}{2}$	2092.6(5)	0.33(12)	6.27	0.215
$\frac{3}{2} \rightleftarrows \frac{7}{2}$	2404.8	0.16(16)	4.36	0.149
$\frac{5}{2} \rightleftarrows \frac{9}{2}$	1245.2(2)	18(6)	51.77	1.773
$\frac{9}{2} \rightleftarrows \frac{11}{2}$	1350.1(4)	10(3)	4.22	0.144

projectile and the target. The calculated quasielastic cross section will be obtained by summing the cross sections of all channels included in the coupling matrix. We start by the investigation of the influence of the projectile in the reaction process. Due to its high excitation energy of 6.02 MeV, the overall effect of coupling the octupole vibration of the first excited state of the ^{16}O is to shift the entire barrier distribution by 0.5 MeV. This is a very well known result [32], which can be taken into account by a renormalization of the bare potential. However, as even at the highest bombarding energy investigated in this work, this state is not strongly excited, in the following calculations we will not include this channel in the coupling scheme. In Table I are listed all pairs of inelastic states of the ^{63}Cu nucleus for which transition probabilities $B(E2)$ are available in the literature.

Several transition probabilities for this nucleus have not yet been reported. The dotted curve in Fig. 2 shows that the coupling of the $5/2^-$ and the $7/2^-$ excited states of the target, with $E^* = 0.962$ MeV and 1.327 MeV, respectively, accounts for most of the increase of the quasielastic cross sections at energies above the Coulomb barrier, when compared with the no-coupling calculations (dashed line). These two channels have similar contributions to this result. It is interesting to observe that the coupled-channels effects start to be important at energies above 32 MeV, when there is energy enough to excite the first excited states of the target. The thin-solid line in Fig. 2 corresponds to the additional coupling of the first excited state, $1/2^-$ and 0.670 MeV and all other excited states presented in Table I (including the intermediate transitions). One can notice that the additional coupling of these several inelastic channels have small importance in the distribution of the reaction cross section in the energy range investigated.

Then, we investigated the influence of the reorientation of the ground-state spin of the target on the other reaction mechanisms. From the static quadrupole deformation value ($Q = -0.211$ b) of the ground-state of the ^{63}Cu and using a quasiparticle vibrational model, its deformation parameter required to reproduce the experimental levels [33] is $\beta_2 = 0.30$. This model was used because this odd-nucleus can be described by a ^{62}Ni vibration core coupled to a proton in the $2p_{3/2}$ level. The deformation parameter predicted by the rotational model is $\beta_2 = 0.27$, which is not used in the present calculations. As shown by the dashed-dotted line in Fig. 2, the inclusion of the ground-state reorientation of the target in the coupling scheme leads to a large increase of the quasielastic cross section above 32 MeV.

The agreement of the CCC with data is still poor at energies 2–3 MeV above the Coulomb barrier. This disagreement could be explained by the lack of several excited states and transfer channels included in the calculations. However, the thick-solid line in Fig. 2 represents the CCC including the most probable transfer channel for this system, as it will be discussed latter in this paper, and shows that the transfer process is unable to take into account the large difference between data and CCC results. So, we believe that this disagreement can be explained by the lack of high excited states included in the calculations, since all coupled channels have low excitation energies, up to 1.86 MeV, corresponding to the $7/2^-_2$ state. The highest excited state described in the literature is the $11/2^-$, with excitation energy of 2.677 MeV. For the high energies investigated in the present work, there is available energy to excite states much higher than the $11/2^-$. So, if one wants to understand into details the reaction mechanisms, it is important that basic nuclear data for stable nuclei, such as $B(E2)$ experimental values, are measured.

The curves in Fig. 3 correspond to the theoretical barrier distributions calculated with the same coupling schemes discussed for Fig. 2. From Fig. 3 one can observe that the good agreement between CCC and data can be reached only up to 30.5 MeV, corresponding to 1 MeV below the main barrier, instead of up to 32 MeV, as observed from the excitation function of Fig. 2. Another important point is that the $5/2^-$ and the $7/2^-$ excited states (and the other inelastic channels) have strong influence in the reaction mechanism even below the energy of the main barrier. It becomes clear from Fig. 3 that when more excited states are included in the CCC, the theoretical prediction approaches the experimental data in the entire energy range investigated. Finally, a very important result that comes out from our analysis of the quasielastic barrier distributions is the striking influence of the ground state reorientation of the ^{63}Cu nucleus on the reaction mechanism at energies around and below the Coulomb barrier. The dashed-dotted line in Fig. 3 shows that, when compared to most of the inelastic channels, the reorientation effect provokes a strong lowering of the maximum of the barrier distribution (the main interaction barrier) and consequently leads to the enhancement of barriers at energies above the Coulomb barrier, between 34 and 37 MeV in Fig. 3, since the total area of the barrier distribution should be unitary.

B. α particle stripping transfer channel

The projectile-like events with $Z = 6$ in the spectra were considered as being α-particle stripping ($Q = -3.43$ MeV). The excitation function for this process, measured at $\theta_{\rm lab} = 161^\circ$, is presented in Fig. 4. One can observe that the transfer

cross sections are very small and, as shown in Figs. 2 and 3, have small influence on the quasielastic reaction mechanism.

The α stripping probability increases with energy up to around 34 MeV, which corresponds approximately to the energy of the Coulomb barrier minus the ground state-to-ground state Q-value of the transfer process. In our calculations, the FRESCO code treats the α-particle as a spin zero particle linked to ^{12}C in the entrance channel and to ^{63}Cu in the exit channel. In the calculations, the nuclear potentials connecting the α-particle to these cores are the conventional Woods-Saxon shape potentials with radius of 1.2 fm, diffuseness parameter of 0.65 fm, and intensities considered as free parameters to fit the experimental levels. All other nuclear potentials used in the calculations (^{16}O-^{63}Cu, ^{12}C-^{63}Cu, ^{12}C-^{67}Ga) were obtained by the SPP double-folding procedure already mentioned. A very important parameter in the CCC is the spectroscopic amplitude to be used. As we measured the total experimental excitation function for this process, from the ground state of the ^{12}C to the ground state and several excited levels of the ^{67}Ga, we were able to evaluate the experimental spectroscopic amplitudes by fitting the data, with the additional assumption that all channels have the same average spectroscopic amplitude (A). The nuclear levels included in the calculations are listed in Table II.

The best fit of the theoretical prediction to the data was obtained with $A = 0.72$ as shown in Fig. 4 by the dotted line, when only transfer channels were coupled. However, the solid line in Fig. 4 shows that the fit becomes much better when the inelastic channels discussed before are included in the coupling matrix. This result shows that the extraction of nuclear parameters from theoretical fits of experimental data is a complex process involving all reaction channels of the system and can be a source of ambiguities. In the present case, despite the better fit obtained with the inclusion of the inelastic channels, the value of the resulting spectroscopic amplitudes did not change significantly.

TABLE II. States of ^{63}Cu and ^{67}Ga considered in the coupled-channels calculations.

^{63}Cu		^{67}Ga	
I^π	E (MeV)	I^π	E (MeV)
$\frac{3}{2}^-$	g.s.	$\frac{3}{2}^-$	g.s.
$\frac{1}{2}^-$	0.669	$\frac{1}{2}^-$	0.167
$\frac{5}{2}^-$	0.962	$\frac{5}{2}^-$	0.359
$\frac{7}{2}^-$	1.327	$\frac{3}{2}^-$	0.828
$\frac{5}{2}^-$	1.412	$\frac{5}{2}^-$	0.911
$\frac{3}{2}^-$	1.547	$\frac{1}{2}^-$	1.082
$\frac{7}{2}^-$	1.861	$\frac{7}{2}^-$	1.202
$\frac{7}{2}^-$	2.093	$\frac{7}{2}^-$	1.412
$\frac{9}{2}^-$	2.208	$\frac{5}{2}^-$	1.554
$\frac{7}{2}^-$	2.405	$\frac{3}{2}^-$	1.639
$\frac{11}{2}^-$	2.677	$\frac{3}{2}^-$	1.809
		$\frac{5}{2}^-$	2.040
		$\frac{3}{2}^-$	2.141
		$\frac{3}{2}^-$	2.172
		$\frac{7}{2}^-$	2.176
		$\frac{3}{2}^-$	3.225

C. Elastic scattering

The elastic scattering for this system has been already measured [26] at energies above the Coulomb barrier. We analyzed those data in order to check the consistency of our calculations. Once again, we will not fit data by changing potential parameters, but instead we compare theoretical predictions with the elastic data. The short-range imaginary potential already used in the calculations was chosen in such way that it does not affect the elastic cross sections. Figure 5 shows a detailed comparison of theoretical predictions with experimental data for the elastic angular distribution at $E_{\text{c.m.}} = 36.7$ MeV, energy for which the effect of the progressive opening of the reaction channels can be easily observed.

Figures 5(a) and 5(b) show the cross sections in linear and logarithmic scales, respectively, in order to facilitate the observation of the results in different angular regions, near the grazing angle or at backward angles. The dotted line is the prediction of CCC when all reaction channels are closed; the dashed line in Fig. 5 represents the coupling of the $1/2^-$ state of the target; the calculation shown by the dashed-dotted line includes the $1/2^-$ and the $5/2^-$ excited states of the target; the thick dotted line is the result of CCC including the three first excited states of the ^{63}Cu nucleus; the thick solid line corresponds to CCC when all excited states of the target for which there are measured $B(E2)$ values are included in the

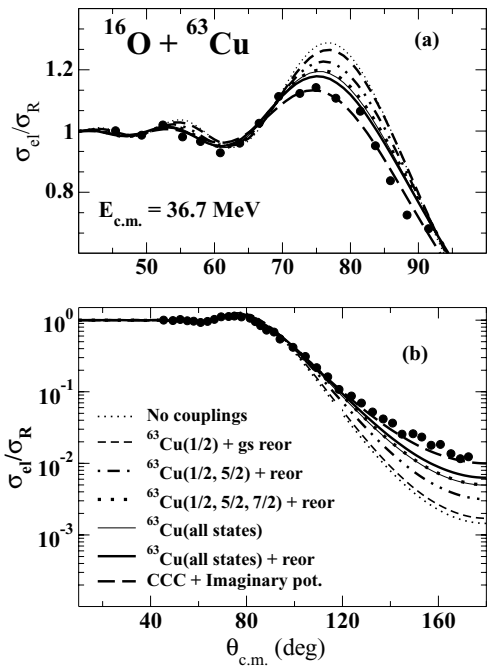

FIG. 5. The experimental elastic angular distribution, at $E_{\text{c.m.}} = 36.7$ MeV [26], presented in (a) linear and (b) logarithmic scales. The curves are the results of coupled-channel calculations and are discussed in the text.

coupling matrix. In all of these theoretical predictions, the reorientation of the ground state of the target was included. In order to show the effect of the reorientation channel in the final result, calculation was performed without reorientation, and its results are shown by the thin solid line in Fig. 5. One can observe that the reorientation effect on the elastic angular distributions for this system is much stronger at backward angles, the same behavior as observed for light projectiles on heavy targets [18–20,23]. We have also investigated the effect of the reorientation of excited states, but this effect has shown to be much less important than with that of the ground state.

It is interesting to investigate into details, from Figs. 5(a) and 5(b), the role of inelastic channels in the elastic scattering. At backward angles, there is a continuous increasing of the elastic cross sections when excited states are progressively coupled. On the other hand, there is a competition between elastic and inelastic scattering around the grazing angle. At angles below the grazing angle (around 90°), the elastic cross section is lowered when the inelastic channels are open. However, for angles above 90°, the overall result of the quantum interference between elastic and inelastic processes is the deviation of a small part of the elastic flux into forward angles. It is important to notice the strong role played by the first three excited states of the target, $1/2^-$, $5/2^-$, and $7/2^-$, which account for most of the total inelastic effects, both below and above the grazing angle. This could be inferred by the high $B(E2)$ values of the transitions involving these three channels, and confirm the strong collectivity of the ^{63}Cu nucleus. The inclusion in the CCC of the other transitions presented in Table I, however, improves the agreement between prediction and data over all angular range. A good agreement, however, is not reached due to the lack of data related to transitions of higher excited states of the target, as already mentioned in the quasielastic analysis. The α-particle stripping channel was also included in the calculations but, due to its very low cross sections, it hardly affects the elastic cross sections.

We performed the same kind of analysis for other six elastic angular distributions at $E_{\mathrm{c.m.}} = 31.1$, 33.9, 35.1, 38.3, 39.9, and 44.7 MeV. The results are presented in Fig. 6, where the dotted lines represent the calculations without any coupling, and the solid lines represent the full CCC including all inelastic transitions listed in Table I. As before, we can observe that the disagreement between theoretical predictions and backward angle data increases at high bombarding energies, because more inelastic channels can be populated and are not taken into account in the coupling scheme.

As already mentioned, it is not our purpose in the present work to fit experimental data, but just as an illustration, we show that we are able to do so if we introduce an imaginary potential to simulate the effect of the channels not included in the CCC. When we introduce a surface imaginary potential, very good agreement could be obtained, as shown in Figs. 5(a), 5(b), and 6 by the large dashed lines. The parameters of the surface imaginary potential used in this case were $V_i = 300$ MeV, $r_i = 0.9$ fm, and $a_i = 0.6$ fm. So, we believe that we have demonstrated that the procedure used in the present work shows that a complete description of reaction mechanisms can not be done without the introduction of an artificial imaginary potential at the interaction region if all

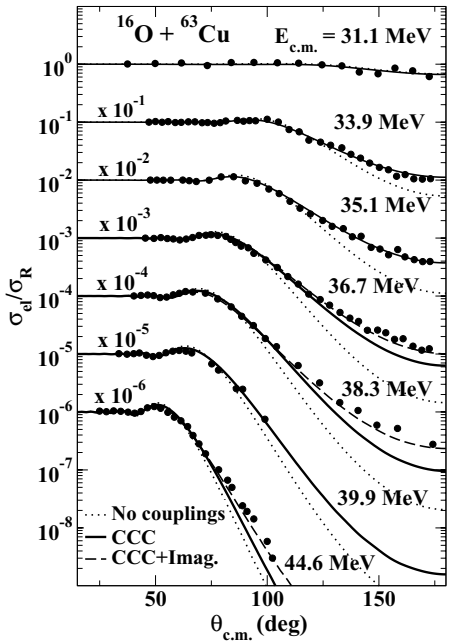

FIG. 6. Seven experimental elastic angular distributions for the ^{16}O + ^{63}Cu system. The curves are the results of coupled-channel calculations and are discussed in the text.

relevant channels are not included in the CCC. Due to the lack of experimental $B(E2)$ values for several high excitation energy states for the target nucleus, this was the situation for the system under investigation in the present work.

IV. SUMMARY AND CONCLUSIONS

Quasielastic excitation function has been measured precisely for the ^{16}O + ^{63}Cu system at a backward angle, at near barrier energies. For the first time, quasielastic barrier distribution has been deduced for a system with a medium odd-A nucleus target, when ground state spin may play an important role in the reaction mechanisms. The α stripping transfer channel excitation function, at the same backward angle, was also measured. Additional data of elastic scattering angular distributions available in the literature for this system were used in the investigation of the role of several individual channels in the reaction dynamics. Full coupled-channels calculations were performed, including several target excited states, without any free parameter, since we used the parameter-free double folding São Paulo potential as bare potential and did not fit the data, but rather compared theoretical predictions with the data. A high collectivity of the ^{63}Cu was observed, mainly due to the strong influence of its $5/2^-$ and $7/2^-$ states on all reaction channels investigated. The procedure used in the present work shows that double-folding potentials are reliable starting point for coupled-channels calculations, and that a complete description of reaction mechanisms can, in principle, be done without the introduction of an artificial imaginary potential at the interaction region. A striking influence of the reorientation of the ground-state target-spin on quasielastic and elastic cross sections was observed. Our analysis also shows the importance of the

quasielastic barrier distribution as a powerful tool in the investigation of reaction mechanisms at energies near the barrier. Finally, we would like to point out that, if one wants to understand into details the reaction mechanisms, it is important that basic nuclear data for stable nuclei, such as $B(E2)$ experimental values for high energy excited states are measured.

ACKNOWLEDGMENTS

The authors wish to thank Prof. M. S. Hussein and Dr. A. Samana for calculating the deformation parameter of the target. This work was supported by CNPq and FAPESP. P.R.S.G. also acknowledges the partial financial support from FAPERJ.

[1] W. Reisdorf, F. P. Hessberger, K. D. Hildenbrand, S. Hofmann, G. Munzenberg, K. H. Schmidt, J. H. R. Schneider, W. F. W. Schneider, K. Summerer, G. Wirth, J. V. Kratz, and K. Schlitt, Phys. Rev. Lett. **49**, 1811 (1982); Nucl. Phys. **A438**, 212 (1985).
[2] M. Beckerman, Rep. Prog. Phys. **51**, 1047 (1988).
[3] S. G. Steadman and M. J. Rhoades-Brown, Annu. Rev. Nucl. Sci. **36**, 649 (1986).
[4] C. H. Dasso *et al*., Nucl. Phys. **A405**, 381 (1983); **A407**, 221 (1983).
[5] R. G. Stokstad, Y. Eisen, S. Kaplanis, D. Pelte, U. Smilansky, and I. Tserruya, Phys. Rev. Lett. **41**, 465 (1978); Phys. Rev. C **21**, 2427 (1980).
[6] D. di Gregorio *et al*., Phys. Lett. **B176**, 322 (1986); Phys. Rev. C **39**, 516 (1989).
[7] P. R. S. Gomes *et al*., Phys. Rev. C **49**, 245 (1994).
[8] N. Rowley *et al*., Phys. Lett. **B254**, 3368 (1991).
[9] M. Dasgupta *et al*., Annu. Rev. Nucl. Part. Sci. **48**, 401 (1998), and references therein.
[10] H. Timmers *et al*., Nucl. Phys. **A584**, 190 (1995).
[11] N. Rowley *et al*., Phys. Lett. **B373**, 23 (1996).
[12] H. Timmers *et al*., Nucl. Phys. **A633**, 421 (1998); H. Timmers *et al*., Phys. Lett. **B399**, 35 (1997).
[13] O. A. Capurro, J. E. Testoni, D. Abriola, D. E. DiGregorio, G. V. Marti, A. J. Pacheco, and M. R. Spinella, Phys. Rev. C **61**, 037603 (2000).
[14] R. F. Simões *et al*., Phys. Lett. **B527**, 187 (2002).
[15] N. Keeley *et al*., Nucl. Phys. **A628**, 1 (1998).
[16] D. S. Monteiro *et al*., Nucl. Phys. **A725**, 60 (2003).
[17] J. F. P. Huiza, E. Crema, D. S. Monteiro, J. M. B. Shorto, R. F. Simoes, N. Added, and P. R. S. Gomes, Phys. Rev. C **75**, 064601 (2007).
[18] G. R. Satchler, Nucl. Phys. **A45**, 197 (1963).
[19] G. R. Satchler, Phys. Lett. **B50**, 309 (1974).
[20] S. E. Hicks and M. T. McEllistrem, Nucl. Phys. **A468**, 372 (1987), and references therein.
[21] V. Hnizdo, K. W. Kemper, and J. Szymakowski, Phys. Rev. Lett. **46**, 590 (1981).
[22] A. T. Rudchik *et al*., Nucl. Phys. **A662**, 44 (2000).
[23] F. Videbaek *et al*., Nucl. Phys. **A256**, 301 (1976).
[24] L. C. Chamon *et al*., Phys. Rev. C **66**, 014610 (2002).
[25] M. A. G. Alvarez *et al*., Nucl. Phys. **A723**, 93 (2003).
[26] L. C. Chamon, Ph.D. thesis, University of São Paulo (1989).
[27] E. Crema, L. C. Chamon, and P. R. S. Gomes, Phys. Rev. C **72**, 034610 (2005).
[28] E. Crema, P. R. S. Gomes, and L. C. Chamon, Phys. Rev. C **75**, 037601 (2007).
[29] J. J. S. Alves *et al*., Nucl. Phys. **A748**, 59 (2005).
[30] A. Diaz-Torres and I. J. Thompson, Phys. Rev. C **65**, 024606 (2002).
[31] I. J. Thompson, Comput. Phys. Rep. **7**, 167 (1988).
[32] K. Hagino, N. Takigawa, M. Dasgupta, D. J. Hinde, and J. R. Leigh, Phys. Rev. Lett. **79**, 2014 (1997).
[33] M. S. Hussein and A. Samana (private communication).